Data-Driven Parameter Inversion for DC Fault Current Analytical Solution of Modular Multilevel Converter-Based High Voltage DC Grid

Meiqin MAO, Xun JIANG, Kaifan HU, and Liuchen CHANG

***Abstract*—In a multi-terminal modular multilevel converter-based high voltage direct current (MMC-HVDC) grid, due to the coupling between converter stations, it is difficult to obtain an accurate analytical solution on the DC fault current through the traditional equivalent resistance-inductance-capacitance circuit model (E-RLCM). In this paper, a data-driven parameter inversion method is proposed to derive the accurate equivalent parameters in the E-RLCM by combining the electromagnetic transient simulation data with the backpropagation neural network, and the polynomial regression. In this way, the accurate analytic calculation expression of the DC fault current for a multi-terminal MMC-HVDC grid with a pole-to-pole fault (PTPF) is obtained. To verify the effectiveness of the proposed method, simulations are performed for a four-terminal MMC-HVDC grid with a PTPF by PSCAD. The results show that the average calculation error of the DC fault current using the inversion parameters is significantly reduced from over 10% to 2.84%.**

***Index Terms*—Backpropagation neural network, data-driven parameter inversion, DC fault current calculation, high voltage direct current grid, modular multilevel converter.**

I. Introduction

MODULAR multilevel converter-based high voltage direct current (MMC-HVDC) grid has the advantages of flexible control of active and reactive power, low harmonic content, and no commutation failure. Therefore, it is expected to be one of the most prospective topologies in the power system dominated by new energy [1].

Due to easy maintenance and low operation cost, overhead lines are usually used in the MMC-HVDC grid [2]. However, they are susceptible to short circuit faults, among which pole-to-pole short circuit faults (PTPS) are the most serious [3]. Because of the small equivalent impedance in the fault circuit after the fault occurs, so the capacitors of the sub-modules will discharge rapidly, and the fault current rising rate can reach the order of 1000 amperes per millisecond after a PTPF occurs. Thus, it is difficult to protect the DC short circuit of the MMC-HVDC grid [4], [5]. Therefore, the analysis and accurate calculation of the DC short-circuit fault current are of great significance for the protection of MMC-HVDC grids.

In the current literature, there is quite some research focused on the DC fault current calculation for the MMC-HVDC grids, which are represented by the frequency-domain equivalent model-based method [6]−[9] and the time-domain equivalent model-based method [10]−[14].

The frequency-domain equivalent model-based method first builds the equivalent model of individual equipment of the MMC-HVDC grid in the frequency domain, for example, the converter station and the coupling line [6], [7]. Subsequently, the frequency-domain equations for DC fault current calculation of the MMC-HVDC grid are derived by combining the equivalent models of individual equipment [8], [9]. Finally, the DC fault current can be calculated precisely and rapidly by solving the frequency-domain equations [6]. In this method, the frequency domain calculation equations of DC fault current are formulated based on thorough consideration of the system characteristics and rigorous analytical derivation, which puts limitations on its application in the DC fault current calculation of complex MMC-HVDC grid.

The time-domain equivalent model-based method linearizes the DC fault circuit loop of the MMC-HVDC grid into an equivalent resistance-inductance-capacitance model (E-RLCM) by some constraints and simplifications, so that an approximate DC fault current can be analytically calculated based on the obtained E-RLCM [10], [11]. In [12], the E-RLCM of a two-terminal MMC-HVDC grid is established. Due to the relatively simple characteristics of the two-terminal MMC-HVDC grid, its equivalent E-RLCM and the corresponding equivalent resistance-inductance-capacitance (RLC) parameters can be accurately determined. In this case, the calculated DC fault current has an extremely high accuracy within 10 ms after the fault occurs, which is of great significance for analyzing the pole-to-pole short-circuit fault current evolution, electrical parameter optimization design, and protection scheme design of two-terminal MMC-HVDC grids.

Manuscript received February 5, 2024; revised May 1, 2024; accepted May 25, 2024. Date of publication September 30, 2024; date of current version June 11, 2024. This work was supported in part by the National Key Research and Development Program of China under the grant No. 2018YFB0904600, and 111 Project under the grant No. BP0719039. *(Corresponding author: Meiqin Mao.)*

M. Mao, X. Jiang, and K. Hu are with Hefei University of Technology, Hefei 230000, China (e-mail: pvcenter@hfut.edu.cn; jaysonxun@163.com; 707631130@qq.com).

L. Chang is with University of New Brunswick, 15 Dineen Dr, Fredericton, New Brunswick E3B 5A3, Canada (e-mail: lchang@unb.ca).

Digital Object Identifier 10.24295/CPSSTPEA.2024.00008

However, a multi-terminal MMC-HVDC grid is more complex. The influence factors of DC fault current include not only the main circuit parameters of the system but also the complicated coupling discharge path of capacitors or control strategies. Therefore, when the E-RLCM is directly applied to a multi-terminal MMC-HVDC grid, its equivalent parameters are difficult to accurately derive from the electrical parameters of the main circuit and transmission lines, resulting in significant calculation errors [13]. To date, some decoupled and split methods are proposed for the calculation of DC fault current on the DC side of the multi-terminal MMC-HVDC grid with PTPF [14], [15]. In these methods, the multi-terminal MMC-HVDC grid is decoupled at certain positions according to the specific structure and fault positions of the multi-terminal MMC-HVDC grid, so that the calculation of DC fault current can be simplified. Although these methods can simplify the analytic derivation and improve the accuracy of the calculation of DC fault current, it still faces the challenge of obtaining accurate equivalent parameters of E-RLCM, which are related to the various factors such as the controller of the converter station, electrical parameters of different MMC-HVDC grids, and different types of fault [16].

The parameter inversion method is often used to predict some parameters in a system model, which are usually difficult to obtain under complex conditions, such as in geology [17], structural engineering [18], etc. In the power system sector, parameter inversion methods are currently used for accurate prediction of equivalent geometrical parameters of transmission lines based on power-frequency parameters [19], calculation of three-phase currents of overhead transmission lines using power-frequency magnetic field data [20], and inversion of the unknown component reliability parameter using the system reliability index and a modified Krawczyk-operator algorithm [21].

However, the parameter inversion methods above strongly rely on mathematical theory support and a lot of mathematical operations, thus, it is difficult to derive accurate inversed parameters.

Artificial intelligence has been booming in recent years. Learning by themselves only through input and output without internal mapping, neural networks can abstract the complex model, save the manual numerical operation of parameter matching cumbersome work, and greatly improve the efficiency of parameter inversion [22]. Thus, it is the future development trend for the parameter inversion problems [23].

So far, a few works have focused on parameter inversion using neural networks, such as using a neural network model for parameter inversion in electromagnetic wave and plasma interaction systems [24] and an electromagnetic inversion model based on the convolutional neural network [25]. But, as far as authors know, in current literature, there is rare work that uses the method of parameter inversion to accurately derive the analytical solution of DC fault current for a multiple-terminal MMC-HVDC grid by combining the data-driven and neural network [26].

This paper proposes a data-driven parameter inversion method to derive an accurate time-domain analytical solution

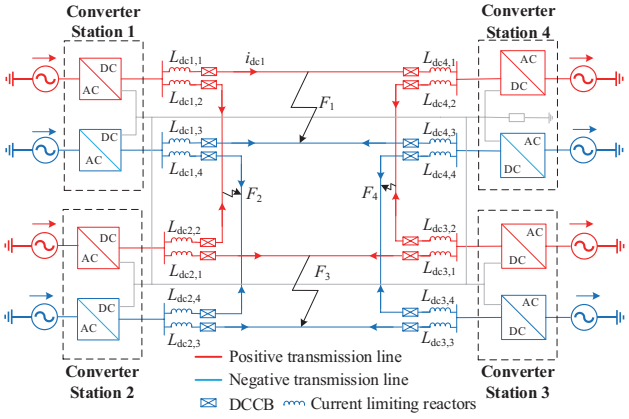

Fig. 1. Topology of the four-terminal MMC-HVDC grid.

expression for the DC fault current of multi-terminal MMC-HVDC grids within 10 ms after a PTPF occurs. In this method, the accurate equivalent RLC parameters of the E-RLCM have been inverted through the electromagnetic transient simulation data-driven and backpropagation neural network (BPNN) method. In addition, the fitting expression between the main circuit parameters of the system and the inversion parameters is further built by the polynomial regression method so that the equivalent RLC parameters can be directly obtained from the known parameters of the multi-terminal MMC-HVDC grid. The contributions of this paper are as follows:

1) A parameter inversion method based on BPNN is initially proposed to solve the inversion problem in the DC fault current accurate analytical solution for MMC-HVDC girds with the PTPFs.

2) By using the electromagnetic transient simulation data-driven and BPNN model, the fitting expression between the main circuit parameters of the MMC-HVDC grid and the inversion parameters for E-RLCM is built by the polynomial regression method, so that the inversion parameters can be directly calculated from the known system parameters.

3) The universal analytical expression of the DC fault current by the proposed method greatly improves the calculation accuracy of the DC fault current of the MMC-HVDC grid.

The arrangement of the rest of the paper is as follows. In Section II, a four-terminal MMC-HDVC grid is taken as an example to show the derivation of its E-RLCM when PTPFs happen. In Section III, the parameter inversion method combining the electromagnetic transient simulation data-driven and BPNN is discussed. In Section IV, simulation results and discussion are provided following conclusions in Section V.

II. Equivalent Circuit for Multi-Terminal MMC-HVDC Grid With Pole-to-Pole Fault

To show how to linearize the fault circuit of the multi-terminal MMC-HVDC grid, the four-terminal MMC-HVDC grid with the PTPFs as in Fig. 1 is used as a case. The topology and parameters of converter stations are referred to [27], which are listed in Table I. $L_{dc,x,y}$ (x, y=1,2,3,4) is the current

TABLE I
PARAMETERS OF THE FOUR-TERMINAL MMC-HVDC-GRID

Parameter	Station 1	Station 2	Station 3	Station 4
Converter rated power/MW	1500	3000	3000	1500
Arm inductance/mH	100	50	50	100
Submodule capacitance/mF	11.2	15	15	8
Number of submodules per arm	228	264	264	284
Control strategy	PQ	PQ	PQ	Vdc
DC voltage/kV	±500			
Current limiting reactor/mH	150			
Neutral inductance/mH	300			

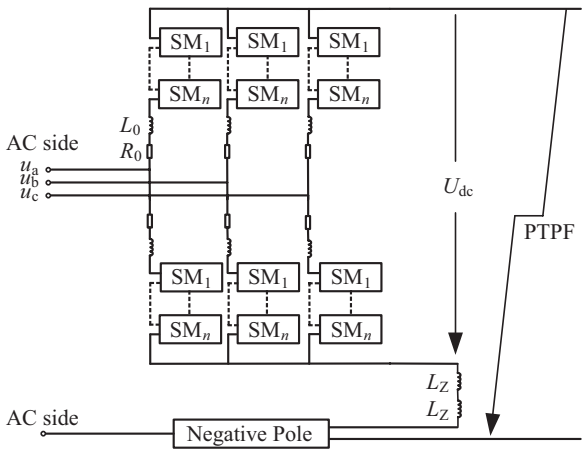

Fig. 2. Structure of MMC converter station.

limiting reactor on different lines. F_1-F_4 represent pole-to-pole short-circuit faults at four different positions, respectively. i_{dc} represents the DC line fault current. In order to avoid component burnout caused by converter stations blocked after faults, the MMC-HVDC grid is often equipped with direct current circuit breaks (DCCBs) at both ends of the DC lines. The DCCBs will cut off the fault lines within 6-10 ms after faults occur to prevent MMCs from being blocked. Therefore, the period of the DC fault currents investigated in this paper is within 10 ms after the occurrence of the faults.

A. E-RLCM for an MMC Converter Station

Fig. 2 shows the topology of the MMC converter station, in which R_0 and L_0 are the equivalent resistance and reactance of each bridge arm, respectively. L_Z is the neutral inductance. U_{dc} is DC voltage. u_a, u_b, u_c represents the AC voltage, respectively. The AC side system is always three-phase symmetric, which does not affect the fault current of the DC side, so the AC side can be ignored [28]. After the fault occurs, the number of input and bypass sub-modules of bridge arms remains unchanged before the converter station is blocked (usually within 10 ms), thus, the converter station can be linearized to an E-RLCM [29], as in Fig. 3.

In Fig. 3, the equivalent R_{sm}, L_{sm}, and C_{sm} can be obtained by (1),

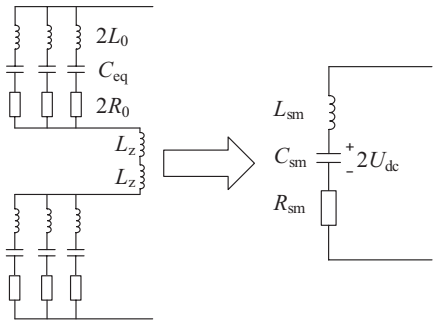

Fig. 3. E-RLCM of one converter station.

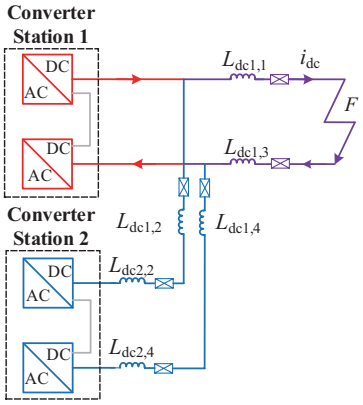

Fig. 4. Simplified fault model of bipolar short circuit fault.

$$\begin{cases} R_{sm} = \dfrac{4}{3} R_0 \\ L_{sm} = \dfrac{4}{3} L_0 + 2L_Z \\ C_{sm} = \dfrac{3}{2} C_{eq} \end{cases} \tag{1}$$

where, C_{eq} is the equivalent capacitance of the phase unit, calculated according to the principle of energy storage equivalence principle [30]. R_{sm}, L_{sm}, and C_{sm} are the equivalent parameters of the equivalent RLC circuit for the converter station with PTPF.

B. E-RLCM for the Four-Terminal MMC-HVDC Grid

Similar to the derivation of E-RLCM for one converter, the whole four-terminal system with a PTPF as in Fig. 1 can also be linearized to E-RLCM. This can be realized through decoupling the fault circuit loop as follows.

For the four terminal MMC-HVDC grid in Fig. 1, the electrical distance between adjacent stations is very large because of the existence of current-limiting reactors in the DC lines. If the short-circuit fault only occurred at F_1, the capacitor discharges in Stations 3 and 4 have an extremely small influence on the fault current at the output terminal of Station 1 and can be ignored. So, only the discharge effects of Stations 1 and 2 need to be considered [14], and the model can be simplified as in Fig. 4. Based on these considerations,

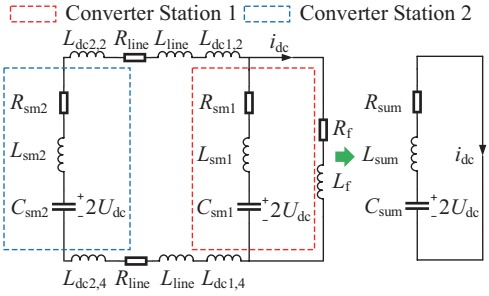

Fig. 5. E-RLCM for the four-terminal MMC-HVDC Grid.

the whole fault circuit can be equivalent to an E-RLCM, as shown in Fig. 5, in which the MMC converter stations have been converted into an equivalent RLC circuit according to the method in the previous Section A.

In Fig. 5, L_{sm}, C_{sm}, and R_{sm} are the equivalent RLC parameters of each converter station. R_{line2} and L_{line2} are equivalent resistance and inductance of the DC transmission line. R_f and L_f are equivalent resistance and inductance of the faulty line, including current limiting reactors $L_{dc1,1}$ and $L_{dc1,3}$, equivalent parameters of the DC line from the outlet of the converter station to the fault point, and fault transition resistance. After linearization, the converter stations and the fault circuit can be linearized to a simple E-RLCM, where R_{sum}, L_{sum}, and C_{sum} are the equivalent RLC parameters, respectively, and can be obtained by (2).

$$\begin{cases} R_{sum} = (R_{sm2} + 2R_{line2}) // R_{sm1} + R_f \\ L_{sum} = (L_{sm2} + 2L_{line2} + L_{dc1,2} + L_{dc2,2} + \\ \qquad L_{dc1,4} + L_{dc2,4}) // L_{sm1} + L_f \\ C_{sum} = C_{sm1} + C_{sm2} \end{cases} \tag{2}$$

According to [31], DC fault current i_{dc} consists of fault component i_f and steady-state component i_0 of capacitor discharge in the converter station. Therefore, only the fault component needs to be calculated and the steady-state component can be added after finding the solution for i_f. The time-domain analytical equation for the fault component if can be easily derived based on the second-order differential equation of the E-RLCM, as in (3) and (4).

$$i_f = \frac{2U_{dc}}{\omega L_{sum}} e^{-\delta t} \sin(\omega t) \tag{3}$$

where,

$$\begin{cases} \delta = \dfrac{R_{sum}}{2L_{sum}} \\ \omega_0 = \dfrac{1}{\sqrt{L_{sum} C_{sum}}} \\ \omega = \sqrt{\omega_0^2 - \delta^2} \end{cases} \tag{4}$$

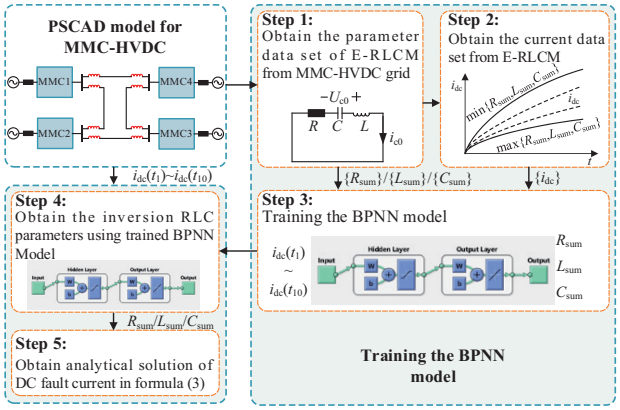

Fig. 6. Proposed parameter inversion method.

It can be seen that the complex four-terminal MMC-HVDC grid with a PTPF can be transformed into E-RLCM through simplification and equivalence. However, a large number of simulation experiments show that the errors between the actual fault current and the current calculated through (1)-(4) may be more than 10% [14]. This is because the equivalent R_{sum}, L_{sum}, and C_{sum} parameters of the fault circuit are difficult to be accurately obtained through (1)-(3) due to the influence of complex main circuit parameters, capacitance discharge coupling of converter stations, and the influence of control algorithms.

III. Parameter Inversion of E-RLCM for the MMC-HVDC Grid

In this paper, the parameter inversion method combining the electromagnetic transient simulation data-driven and BPNN is proposed to inverse the RLC parameters of the E-RLCM.

A. Proposed Parameter Inversion Method

The proposed parameter inversion method is shown in Fig. 6, which includes the following main steps.

Step 1: Obtain the equivalent RLC parameter data set

Firstly, the E-RLCM of a specific MMC-HVDC grid is built in PSCAD/EMTDC according to the following principles:

1) According to the analysis above, only the fault component of i_{dc} is calculated. Thus, the initial current of the E-RLCM is set as zero, and the initial capacitor voltage is set to $2U_{dc}$ according to the equivalent circuit in Fig. 4 and Fig. 5.
2) Taking (1) and (2) as a reference, practical engineering requirements are also considered. The ranges of R_{sum}, L_{sum}, and C_{sum} in the E-RLCM are estimated. In this process, the variation range of the R_{sum}, L_{sum}, and C_{sum} should be designed to include all feasible parameter value ranges, so that the obtained parameter inversion model can be applied to the MMC-HVDC grid with different system parameters. Taking the case shown in Fig. 1 as an example, the corresponding R_{sum}, L_{sum}, and C_{sum} in the E-RLCM are estimated among the ranges of 10 Ω-30 Ω, 0.1 H-1 H and 200 μF-2000 μF, respectively. One thousand groups of R_{sum}, L_{sum}, and C_{sum} parameters are randomly sampled within these ranges as the equivalent RLC parameter data set.

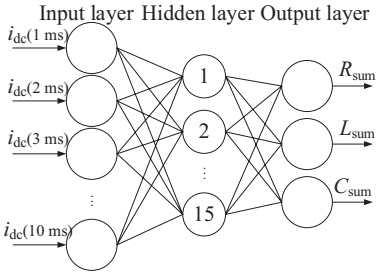

Fig. 7. BPNN model.

The estimated range of R_{sum}, L_{sum}, and C_{sum} parameters discussed above is only used as a reference for selecting the equivalent RLC parameters data set. In practice, the variation ranges of equivalent RLC parameters should be chosen in a larger range, so that the characteristics of the DC fault current of the original MMC-HVDC grid can be thoroughly covered. It's worth noting that it is difficult to estimate the range of equivalent RLC parameters by (2) for more complex MMC-HVDC grids with more than four terminals. In this case, the variation range of the equivalent RLC parameters should be extended to larger ranges so that the fault characteristics of the complex MMC-HVDC grids can be well-trained in the following steps.

Step 2: Obtain the fault current training data set

Sweeping the equivalent R_{sum}, L_{sum}, and C_{sum} parameters parameter data set obtained in Step 1, the corresponding fault current data set is obtained by performing simulations on the E-RLCM in PSCAD.

Step 3: Training BPNN

1) Input and output settings of BPNN: The structure of BPNN adopted in this paper is shown in Fig. 7. The inputs of BPNN are the sampling values of the fault current at 1 ms, 2 ms..., and 10 ms, and the outputs are equivalent parameter values of corresponding R_{sum}, L_{sum}, and C_{sum} parameters of the E-RLCM obtained in Step 1. Its loss function is shown as in (5).

$$E=\frac{1}{2N}\sum_{i=1}^{N}(x_i-y_i)^2 \tag{5}$$

where E is the error, x_i is the real value of the inversed R_{sum}, L_{sum}, and C_{sum} parameters, y_i is the output of the BPNN, and N is the number of samples.

2) Training BPNN model: A total of 5000 sets of input DC fault current and output reversed R_{sum}, L_{sum}, and C_{sum} parameters data obtained through Step 2 are used to train the BPNN model, of which the first 70% was used as the training set, 15% as the test set, and 15% as the verification set. To improve the generalization ability of the obtained BPNN model, the BPNN model can be updated online with the newly sampled DC fault current data set.

Step 4: Acquisition of the inversion RLC parameters

The electromagnetic transient simulation data for the DC fault current of the actual four-terminal MMC-HVDC grid are fed as the input of the obtained BPNN model. The output R_{sum}, L_{sum}, and C_{sum} parameters of the corresponding E-RLCM can be regarded as the inversed equivalent RLC parameters of the MMC-HVDC grid.

Step 5: Analytical solution of DC fault current

The analytical solution expression of the DC fault current can be obtained by substituting the inversed R_{sum}, L_{sum}, and C_{sum} parameters into (3).

B. Regression of Inversed Parameters and System Parameters

Based on the inversed equivalent RLC parameters obtained in the previous Section A, the unified mapping relationship between the inversed equivalent RLC parameters and the actual main circuit parameters of the four-terminal MMC-HVDC grid is further built, so that the equivalent RLC parameters can be directly calculated by the mathematical relationship with known system parameters, and then the accurate analytical equation of the DC fault current can be derived.

In this paper, the regression equations between the actual main circuit parameters and the inversed equivalent RLC parameters are built by polynomial regression, and the procedure is discussed as follows.

Prior to the regression, the correlation between equivalent RLC parameters and actual main circuit parameters is investigated to identify the actual main circuit parameters which are strongly correlated with the equivalent RLC parameters. Therefore, when formulating the regression equations for R_{sum}, L_{sum}, and C_{sum}, only the main circuit parameters with strong correlation are considered to simplify the regression equations. Taking the main circuit parameters of the system in Fig. 5 as the analysis object, R_{sm1}, and R_{sm2} are the on-resistances of the power switch devices of the sub-modules, which are generally very small and can be ignored. Meanwhile, L_{dc1}, L_{dc2}, and L_{line} with series relationship are combined into L_{line} in this paper, so a total of 8 system parameters need to be analyzed in correlation analysis.

During the correlation analysis, 32 groups of orthogonal experiments are designed. Different actual main circuit parameter values are set for each group of experiments to obtain the corresponding DC fault current data. Thereby, the corresponding inversed equivalent RLC parameters can be obtained through the trained BPNN model. The correlation between equivalent RLC parameters and actual main circuit parameters is quantified by the significance value P, as in (6), which is calculated based on the SPSS software. When P is less than 0.05, it indicates that there is a significant correlation between the two variables.

$$P=\frac{\mathrm{cov}(X,Y)}{\sqrt{\mathrm{var}(X)\cdot\mathrm{var}(Y)}} \tag{6}$$

where X and Y are variables like R_{sum} and L_{line}. cov(*X, Y)* is the covariance of X and Y, var(X) is the variance.

The significance values P for different inversed equivalent RLC parameters versus different actual main circuit parameters of the four-terminal MMC-HVDC grid are shown in Table II.

TABLE II
SIGNIFICANCE ANALYSIS RESULTS OF INVERSION PARAMETERS

System parameters	R_{sum}	P-value L_{sum}	C_{sum}
L_{line}	0.004	0.000	0.001
R_{line}	0.495	0.531	0.848
L_{sm1}	0.000	0.000	0.000
L_{sm2}	0.611	0.961	0.422
C_{sm1}	0.000	0.916	0.188
C_{sm2}	0.109	0.979	0.933
L_f	0.000	0.000	0.000
R_f	0.046	0.096	0.266

As can be seen from Table II, the inversed parameter R_{sum} is significantly correlated with the actual main circuit parameters L_{line}, L_{sm1}, C_{sm1}, L_f, and R_f, while the inversed parameters L_{sum} and C_{sum} are significantly correlated with the actual main circuit parameters L_{line}, L_{sm1}, and L_f.

According to the above analysis, the actual main circuit parameter with higher P values is considered. The polynomial regression equation for the E-RLCM is derived as follows:

$$\begin{cases} R_{sum} = \boldsymbol{A}(\boldsymbol{L}_{line}, \boldsymbol{L}_{sm1}, \boldsymbol{C}_{sm1}, \boldsymbol{L}_f, \boldsymbol{R}_f)^T + p_1 \\ L_{sum} = \boldsymbol{B}(\boldsymbol{L}_{line}, \boldsymbol{L}_{sm1}, \boldsymbol{L}_f)^T + p_2 \\ C_{sum} = \boldsymbol{C}(\boldsymbol{L}_{line}, \boldsymbol{L}_{sm1}, \boldsymbol{L}_f)^T + p_3 \end{cases} \tag{7}$$

where $\boldsymbol{A}$, $\boldsymbol{B}$, and $\boldsymbol{C}$ are the coefficient matrices. p_i is constant (i=1,2,3). $\boldsymbol{L}_{line} = (L_{line}, L_{line}^2, L_{line}^3)$, $\boldsymbol{C}_{sm1} = (C_{sm1}, C_{sm1}^2, C_{sm1}^3)$, $\boldsymbol{L}_f = (L_f, L_f^2, L_f^3)$, $\boldsymbol{R}_f = (R_f, R_f^2, R_f^3)$, $\boldsymbol{L}_{sm1} = (L_{sm1}, L_{sm1}^2, L_{sm1}^3)$.

In (7), only the first three orders of the actual main circuit parameters are taken into account, which is sufficient to accurately fit the relationship between the inversed equivalent RLC parameters and the actual main circuit parameters. The coefficient matrices $\boldsymbol{A}$, $\boldsymbol{B}$, $\boldsymbol{C}$, and p_i can be derived by polynomial regression methods when inversed R_{sum}, L_{sum}, C_{sum}, and $\boldsymbol{L}_{line}$, $\boldsymbol{C}_{sm1}$, $\boldsymbol{L}_f$, $\boldsymbol{R}_f$, $\boldsymbol{L}_{sm1}$ are known. Similar to the data set obtaining process in Section III-A, different scenarios with different inversed equivalent RLC parameters and actual main circuit parameters should be thoroughly considered so that the obtained regression equation is suitable for the real MMC-HVDC grids with different main circuit parameters.

In this paper, considering the constraints of stable operation, the ranges of the main circuit parameter of the four-terminal MMC-HVDC grid are designed as shown in Table III.

IV. SIMULATION RESULTS AND DISCUSSIONS

A. Parameter Inversion

In this paper, the proposed data-driven parameter inversion method is validated based on the four-terminal MMC-HVDC grid in Fig. 1. The detailed system parameters are presented in Table I, which will not repeat here.

Fig. 8 shows the training performance of the BPNN model. It can be seen that the mean square error of the training results reaches a minimum of about 0.009 at the 953 epochs.

TABLE III
RANGES FOR RLC PARAMETERS IN MAIN CIRCUIT

System parameters	Value range
L_{line}	0.2-0.8 H
R_{line}	0.3-0.6 Ω
L_{sm1}	0.1-0.4 H
L_{sm2}	0.1-0.4 H
C_{sm1}	8-12 mF
C_{sm2}	8-12 mF
L_f	0.1-0.4 H
R_f	0.3-0.6 Ω

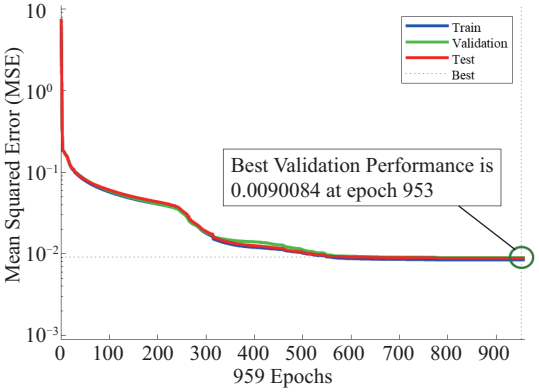

Fig. 8. Performance of neural network training.

TABLE IV
INVERSED RLC PARAMETERS

Inversed parameters	Value
R_{sum}	10.99 Ω
L_{sum}	0.204 H
C_{sum}	0.412 mF

To test the trained BPNN model, a group of electromagnetic transient simulation data for the DC fault current of the four-terminal MMC-HVDC grid is fed into the obtained BPNN model. The inversed equivalent RLC parameters can be obtained as shown in Table IV. Based on the obtained R_{sum}, L_{sum}, and C_{sum}, the DC fault current can be calculated according to (3). The comparison of calculated DC fault current and PSCAD-based simulation results is shown in Fig. 9. The error of the DC fault current at 10 ms after the fault occurs is only 0.77%, which is much smaller than the 10% in [14].

B. Regression Results of Inversed Parameters and System Parameters

A total of 160 groups of DC fault current data are obtained by varying the corresponding R_{sum}, L_{sum}, and C_{sum} parameter values within the ranges given in Table II for the four-terminal MMC-HVDC grid in PSCAD. The DC fault current data is input into the trained BPNN model to obtain the inversed equivalent RLC parameters. Through the polynomial regression method, the corresponding regression equations between main circuit parameters and inversion parameters are

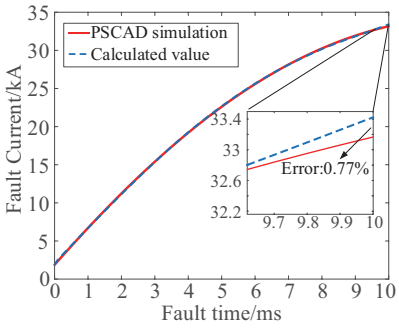

Fig. 9. Calculated DC short-circuit fault current with inversed parameters.

obtained as in (8).

$$\begin{cases} R_{\text{sum}} = -0.101\times L_{\text{line}} + 20.835\times L_{\text{sm1}} + 35.188\times L_{\text{f}} - \\ \qquad 547.701\times C_{\text{sm1}} + 1.118\times R_{\text{f}} + 9.45 \\ L_{\text{sum}} = 0.133\times L_{\text{line}} + 1.144\times L_{\text{sm1}} + 2.012\times L_{\text{f}} + 0.038 \\ C_{\text{sum}} = 0.00265\times L_{\text{line}} - 0.0153\times L_{\text{sm1}} - 0.00317\times \\ \qquad L_{\text{f}} + 0.0262\times {L_{\text{sm1}}}^2 - 0.00046\times {L_{\text{line}}}^2 + \\ \qquad 0.00246\times {L_{\text{f}}}^2 - 0.004\times L_{\text{line}} L_{\text{sm1}} - 0.0044\times \\ \qquad L_{\text{line}} L_{\text{f}} + 0.0188\times L_{\text{sm1}} L_{\text{f}} + 0.00171 \end{cases} \tag{8}$$

The comparison between the R_{sum}, L_{sum}, and C_{sum} parameters calculated by the final regression equations and the inversion parameters of the R_{sum}, L_{sum}, and C_{sum} is shown in Fig. 10.

As in Fig. 10, there is only a small error between the regression values and the inversion values. It indicated that the fitting accuracy is high, and (8) can be used for actual fault current calculation. By substituting (8) into (3) and (4), the analytical solution expression for the DC fault current of the four-terminal MMC-HVDC grid with PTPF can be obtained based on the combination of BPNN and the parameter inversion method.

C. Simulation Verification

In this section, the calculated DC fault currents based on the proposed method are compared with the simulation values of PSCAD, so that the accuracy of the proposed method with different fault locations and system parameters can be verified.

Based on the PSCAD model of the four-terminal MMC-HVDC grid in Fig. 1, the pole-to-pole short-circuit faults are set at positions F_1~F_4, and the corresponding DC fault currents of these four pole-to-pole short-circuit faults are denoted as i_{dc1}, i_{dc2}, i_{dc3}, and i_{dc4}, respectively.

The system parameters of the MMC-HVDC grid are changed according to Table V, in which four different sets of parameters were designed. The calculated DC fault currents are compared with the simulation values over these four sets of parameters at each fault position, as shown in Fig. 11.

Table VI shows the absolute errors of DC fault currents between PSCAD simulation values and calculated values within the time of 10 ms after the faults occur. Meanwhile, the absolute errors of DC fault currents with the traditional method in [14] have also been presented in Table VI for comparison.

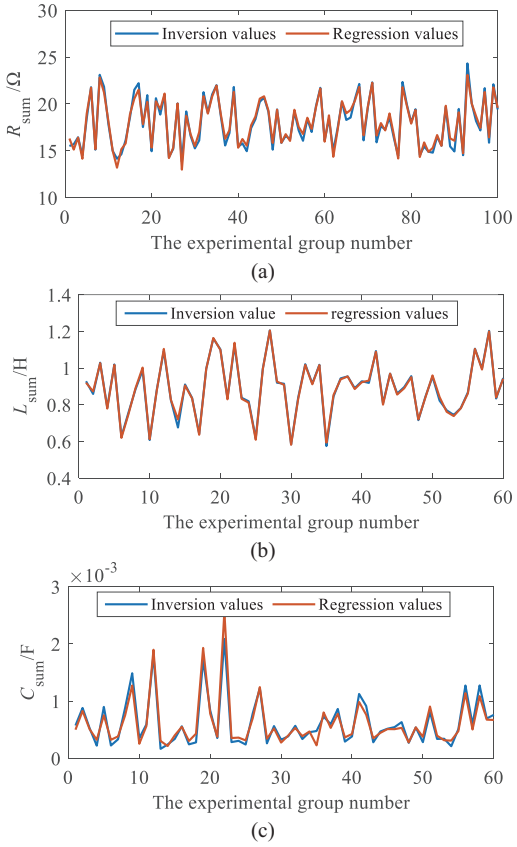

Fig. 10. Comparison between the regression values and the inversion values. (a) Parameter R_{sum}. (b) Parameter L_{sum}. (c) Parameter C_{sum}.

TABLE V
EXPERIMENTAL SETTINGS

System parameters	Parameters values			
	Test 1	Test 2	Test 3	Test 4
L_{line}/H	0.2	0.8	0.6	0.8
R_{line}/Ω	0.3	0.4	0.3	0.6
L_{sm1}/H	0.4	0.3	0.2	0.1
L_{sm2}/H	0.4	0.1	0.3	0.3
C_{sm1}/mF	9.5	9.5	9.5	11.5
C_{sm2}/mF	8.5	9.5	11.5	8.5
L_{f}/H	0.2	0.4	0.4	0.4
R_{f}/Ω	0.4	0.4	0.3	0.4

From the above comparison results, it can be seen that the calculation results of fault current with inversion parameters are very close to the simulation results of the PSCAD model, with a maximum error of 7.00%, a minimum error of 0.15% and an average error of 2.84%. Considering that there are some errors in the inversion parameter values fitted by polynomial regression, the error fluctuation of the calculated fault current value is large, but the average error is small in general. Compared with the existing methods in [14], there is a relatively better error performance for most of the system parameters. Therefore, the proposed calculation method has higher accuracy and versatility, it is suitable for the four-terminal MMC-HVDC grid with various system parameters.

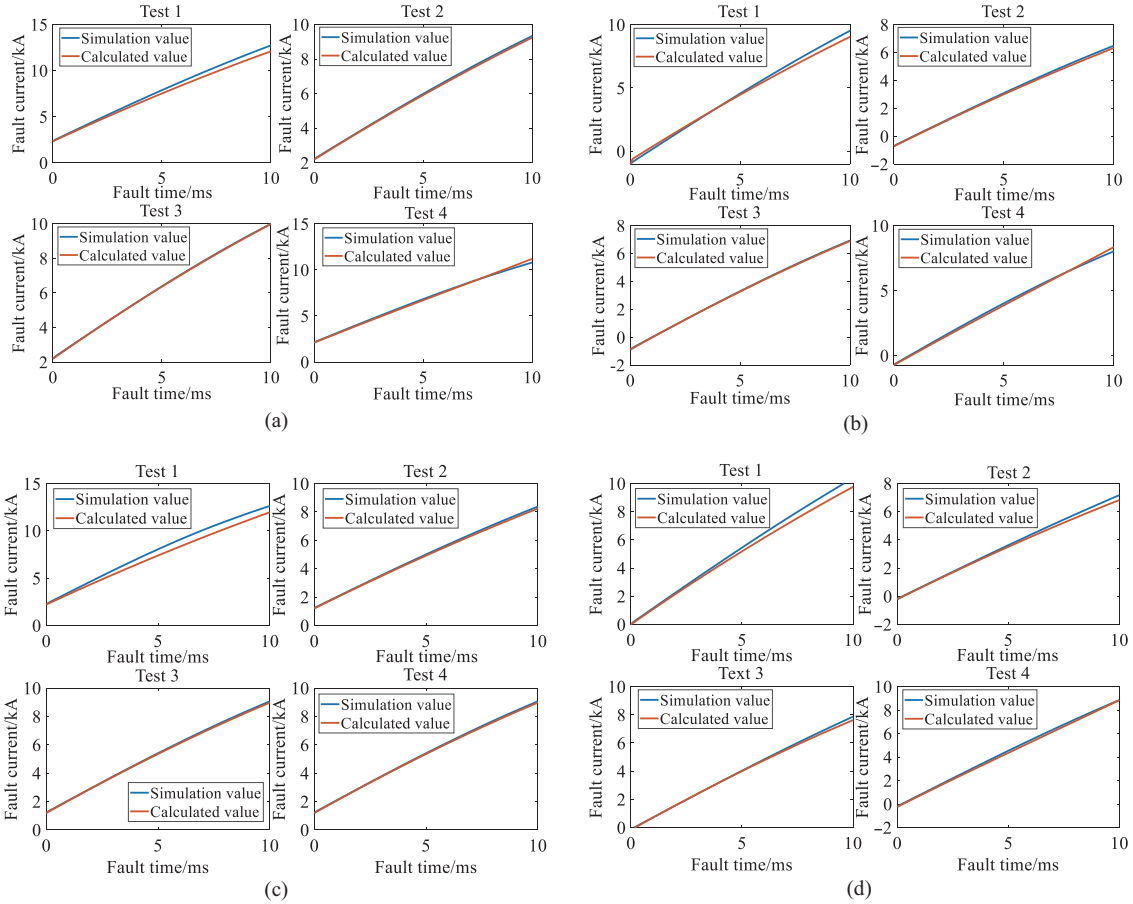

Fig. 11. Comparison between calculation values and simulation values of the DC fault current. (a) Fault current i_{dc1} with F_1. (b) Fault current i_{dc2} with F_2. (c) Fault current i_{dc3} with F_3. (d) Fault current i_{dc4} with F_4.

TABLE VI
COMPARISON OF EXPERIMENTAL RESULTS

Fault current	Test 1	Test 2	Test 3	Test 4	Traditional Method in [14]
i_{dc1}	5.02%	1.02%	0.15%	3.66%	11.63%
i_{dc2}	5.04%	2.54%	0.56%	4.06%	--
i_{dc3}	7.00%	0.63%	0.61%	4.38%	6.05%
i_{dc4}	5.24%	1.64%	1.01%	2.92%	4.40%

V. CONCLUSION

In this paper, the parameter inversion problem of the E-RLCM is formulated for the DC fault analytical solution of the MMC-HVDC grid with PTPFs. This parameter inversion problem is solved by taking advantage of the rich electromagnetic transient simulation data from the MMC-HVDC grid by PSCAD, BPNN, and polynomial regression. The inversion parameters of the improved E-RLCM for the MMC-HVDC grid with PTPFs can be finally mapped to the known main circuit parameters, and then the analytical expression of the DC fault current versus the main circuit parameters can be derived. The simulation results for the four-terminal MMC-HVDC grid with PTPFs show that the average error of the DC fault current calculated by the proposed method is only 2.84%, which is significantly lower than that by the traditional methods. Therefore, the proposed method is valuable to the practical application of the MMC-HVDC grids.

Future work can further focus on the reduction of the calculation error of the DC fault current by improving the regression accuracy of inversion parameters. Meanwhile, the interpretability of the proposed method is urgently to be improved so that it can be applied to the mechanism analysis of fault current evolving.

REFERENCES

[1] G. Tang, Z. He, and H. Pang, "Research, application and development of VSC-HVDC engineering technology," in *Automation of Electric Power Systems*, vol. 37, no. 15, pp. 3–14, Aug. 2013.

[2] Z. Xu, Y. Xue, and Z. Zhang, "VSC-HVDC technology suitable for bulk power overhead line transmission," in *Proceedings of the CSEE*, vol. 34, no. 29, pp. 5051–5062, Oct. 2014.

[3] J. Candelaria and J. -D. Park, "VSC-HVDC system protection: A review of current methods," in *2011 IEEE/PES Power Systems Conference and Exposition*, Phoenix, AZ, USA, 2011, pp. 1–7.

[4] C. Zhang, G. Song, and X. Dong, "Principle of non-unit traveling wave protection for VSC-HVDC transmission line using fault current initial traveling wave fitting," in *Proceedings of the CSEE*, vol. 41, no. 8, pp. 2651–2661, Apr. 2021.

[5] H. Yang, W. Wang, L. Jing, and X. Wu, "Analysis on transient characteristic of DC transmission line fault in MMC based HVDC transmission system," in *Power System Technology*, vol. 40, no. 1, pp.

40–46, Jan. 2016.
[6] B. Li, W. Wang, B. Li, Y. Liu, W. Wen, and X. Chen, "Research on a current calculation method and characteristics of pole-to-ground faults in true bipolar MMC-HVDC grids considering line coupling," in *Electric Power Systems Research*, vol. 192, pp. 1–13, Mar. 2021.
[7] B. Li, X. Jiao, W. Wen, W. Wang, and B. Li, "Study on calculation method for steady-state short-circuit current of MMC during a DC pole-to-pole fault," in *IEEE Transactions on Power Delivery*, vol. 37, no. 4, pp. 2492–2502, Aug. 2022.
[8] C. Li, C. Zhao, J. Xu, Y. Ji, F. Zhang, and T. An, "A pole-to-pole short-circuit fault current calculation method for DC grids," in *IEEE Transactions on Power Systems*, vol. 32, no. 6, pp. 4943–4953, Nov. 2017.
[9] S. Zhu, C. Zhao, C. Li, and J. Xu, "The DC fault current calculation of DC fault current limiter action included in bipolar MMC-HVDC grid," in *Proceedings of the CSEE*, vol. 39, no. 2, pp. 469–478, Jan. 2019.
[10] N. Liu, L. Ning, D. Wu, Y.Su, H. Teng, and L. Gao, "Analysis and protection of DC short circuit fault in true bipolar MMC-HVDC system," in *2019 4th Asia Conference on Power and Electrical Engineering (ACPEE 2019)*, Hangzhou, China, 2019, pp. 28–31.
[11] H. Yang and H. Zeng, "Modeling on transient characteristic and suppression control of DC fault in MMC-HVDC system," in *IOP Conference Series: Materials Science and Engineering*, vol. 394, no. 4, p. 042117, Apr. 2018.
[12] J. Chen, C. Sun, G. Li, L. Yang, and L. Jiang, "Study on characteristics of DC fault in bipolar MMC-HVDC system," in *Transactions of China Electrotechnical Society*, vol. 32, no. 10, pp. 53–60, May. 2017.
[13] L. Tang and X. Dong. "An approximate method for the calculation of transmission line fault current in MMC-HVDC grid." in *Proceedings of the CSEE*, vol. 39, no. 2, pp. 490–498, Jan. 2019.
[14] L. Hao, W. Li, and Z. Wang, "Practical calculation for bipolar short-circuit fault current of transmission line in MMC-HVDC grid," in *Automation of Electric Power Systems*, vol. 44, no. 5, pp. 68–76, Mar. 2020.
[15] Y. Liu, M. Mao, L. Chang, and Z. He, "Analytical calculation of pole-to-pole short circuit fault current in MMC-HVDC-Grid," in *2021 IEEE 1st International Power Electronics and Application Symposium (PEAS)*, Shanghai, China, 2021, pp. 1–6.
[16] L. Wu, M. Mao, and Y. Shi, "Analytical calculation of DC short-circuit fault current of modular multi-level converter-HVDC grid with active current limiting control," in *Transactions of China Electrotechnical Society*, vol. 39, no. 3, pp. 785–797, Feb. 2024.
[17] Z. Ren and T. Kalscheuer, "Uncertainty and resolution analysis of 2D and 3D inversion models computed from geophysical electromagnetic data," in *Surveys in Geophysics*, vol. 41, pp. 47–112, Jan. 2020.
[18] J. Wang, Q. Duan, and S. Ji, "Research progress of field measurements and inversion methods of ice loads on ship structure during ice navigation," in *Advances in Mechanics*, vol. 50, no. 1, pp. 94–123, Jan. 2020.
[19] B. Li and M. Lv, "A calculation method of transmission line equivalent geometrical parameters based on power-frequency parameters," in *International Journal of Electrical Power and Energy Systems*, vol. 111, pp. 152–159, Oct. 2019.
[20] D. Xiao, K. Jiang, and H. Liu, "Inversion method for calculating three-phase currents of overhead transmission lines by using power-frequency magnetic field data," in *Proceedings of CSEE*, vol. 36, no. 5, pp. 1438–1444, Mar. 2016.
[21] B. Hu, K. Xie, and H. Tai, "Inverse problem of power system reliability evaluation: Analytical model and solution method," in *IEEE Transactions on Power Systems*, vol. 33, no. 6, pp. 6569–6578, Dec. 2018.
[22] C. Pinzon, K. Hasewaga, and H. Murakawa, "Artificial neural network application for parameter prediction of heat induced distortion," in *IEA/AIE 2016*, vol. 9799, pp. 599–608, Jul. 2016.
[23] L. Wang, M. zhang, and H. Zhu, "Review on artificial neural networks and their applications in geoscience," in *World Nuclear Geoscience*, vol. 38, no. 1, pp. 15–26, Mar. 2021.
[24] Y. Zhang, H. Fu, and Y. Sui, "Neural network model for parameter inversion in electromagnetic wave and plasma interaction systems," in *IEEE Transactions on Plasma Science*, vol. 48, no. 6, pp. 2143–2152, Jun. 2020.
[25] F. Tian, Y. Yang, and L. Mao, "Electromagnetic inversion algorithm based on convolutional neural network," in *2020 Cross Strait Radio Science & Wireless Technology Conference (CSRSWTC)*, Fuzhou, China, 2020, pp. 1–3.
[26] K. Hu, M. Mao, and L. Chang, "Parameters inversion of equivalent RLC fault circuit for MMC-HVDC grid based on BP neural network," in *2021 IEEE 5th Conference on Energy Internet and Energy System Integration (EI2)*, Taiyuan, China, 2021, pp. 966–971.
[27] Y. Xue and Z. Xu, "On the bipolar MMC-HVDC topology suitable for bulk power overhead line transmission: configuration, control, and DC fault analysis," in *IEEE Transactions on Power Delivery*, vol. 29, no. 6, pp. 2420–2429, Dec. 2014.
[28] Z. Xu, H. Xiao, and Z. Zang, Flexible HVDC transmission system, Beijing: China Machine Press, 2017.
[29] X. Guo, X. Cui, and L. Qi, "DC short-circuit fault analysis and protection for the overhead line bipolar MMC-HVDC system," in *Proceedings of the CSEE*, vol. 37, no. 8, pp. 2177–2185, Apr. 2017.
[30] Z. Xu, H. Xiao, and L. Xiao, "DC fault analysis and clearance solutions of MMC-HVDC systems," in *Energies*, vol. 11, no. 4, pp. 941–952, Apr. 2018.
[31] Z. Zhang, "Research on several issues in MMC-HVDC for overhead line transmission," Hangzhou: Zhejiang University, 2016.

Meiqin Mao received the B.Sc., M.Sc. and Ph.D. degree in electrical engineering from Hefei University of Technology in 1983, 1988, and 2004 respectively. She is now a Professor with School of Electrical and Automation Engineering, Hefei University of Technology, China. And her research interests include renewable energy generation technology, distributed power generation and microgrids, power electronics applied in power system. She has published more than 200 journal/conference technical papers. She now serves as an Associate Editor for *IEEE Journal of Emerging and Selected Topics in Power Electronics*.

Xun Jiang was born in Hefei, China, on Sept. 23, 1995. He received a B.Sc. degree in the school of electrical engineering from Anhui Polytechnic University in 2017. He is currently working toward a Ph.D. degree in electrical engineering at Hefei University of Technology. His research interests include renewable energy integrated power system stability analysis and control, active power decoupling technical for single-phase PV inverter. He is the post Chair of IEEE PELS Student Branch Chapter at Hefei University of Technology (2022-2024).

Kaifan Hu received the B.Sc. degree in electrical engineering and automation from Shihezi University, Xinjiang, China, in 2019, the M.Sc. degree in electrical engineering from Hefei University of technology in 2022. He is currently working as an Engineer at State Grid Bengbu Electric Power Supply Company. His research interests include HVDC system failure calculation and analysis.

Liuchen Chang received the B.Sc. degree from Northern Jiaotong University, Beijing, China, in 1982, the M.Sc. degree from the China Academy of Railway Sciences, Beijing, China, in 1984, and the Ph.D. degree from Queen's University, Kingston, ON, Canada, in 1991. He is Professor of electrical and computer engineering and NSERC Chair in Environmental Design Engineering at the University of New Brunswick, Fredericton, NB, Canada. He is a Fellow of Canadian Academy of Engineering. His principal research interests and experience include distributed power generation, renewable energy, analysis and design of electrical machines, variable speed drives, finite-element electromagnetic analysis and design, power electronics, and EV traction system.